Genetic Algorithms for MRI Magnet Design

Nicholas R. Shaw and Richard E. Ansorge

[1]*Abstract*--**Continuing advances in the field of parallel computing have allowed non-linear optimization techniques to be applied to many problems previously considered too computationally demanding. We describe a general magnet design software package, CamGASP, which uses Genetic Algorithms (GAs) for the design of large whole-body MRI systems. The method of GAs allows a population of many designs to evolve with a bias towards the fittest designs continuing to later generations. Central to all non-linear optimization techniques is the cost function, which decreases for designs that match the required specifications and are hence deemed to be "fitter". Multiple evaluations of the cost function are necessary to complete a single generation and this task can readily be shared across a network of processors, working in parallel. Thus GAs are especially suited to running on parallel computer systems. We present results of the performance of the GA software and also discuss methods for rapid calculation of magnetic fields from circular coils. We also present specific superconducting MRI magnet designs including a split coil optimized for simultaneous PET and MRI.**

Index Terms-- **Combined PET/MRI, Genetic algorithm, magnet design, parallel computing.**

I. Introduction

PRELIMINARY results on using Genetic Algorithms to optimize the design of a large whole body MRI magnet have been reported by us [1]. In this paper we describe the methods and results obtained using a new software suite, CamGASP (Cambridge Genetic Algorithm Software Package). The new software has much improved magnetic field calculations, a more flexible Genetic Algorithm and a better user interface. Particular care is required when calculating magnetic fields near coil boundaries to preserve accuracy and computational efficiency. The final section of the paper presents two novel MRI magnet designs obtained with our method. The first is a short whole body magnet with a 1 m bore depth and 1 m bore diameter, the second is a split coil MRI magnet optimized as part of a novel combined PET/MRI system.

II. Methods

A. Genetic Algorithms

The method of GAs has been described in our previous paper and elsewhere [2]. In magnet design work, individual coils are treated as separate entities and classed as 'genes'. A chromosome is then made up from all the genes, and constitutes the complete magnet design. A population size of 128 designs was found to be suitable and used for the calculations described here. Each generation undergoes a series of operations including selection, recombination, mutation and replacement. Our code also implements more advanced GA techniques to improve performance. These include niching, where several sub-populations are allowed to evolve in separate environments (similar to the Galapagos islands) with each one finding a different local minimum. After a defined number of generations, cross migration between the niches may be allowed, depending on the specific implementation used.

Variable parameters can also be used to control the genetic algorithm. Genetic mutation rates and mating probabilities can all be changed during the course of the optimization as the algorithm converges on a stationary point. Other approaches to genetic algorithms use a variable population size, with the 'fitter' or better individuals surviving for longer and passing their genes on to more generations. Each of these additions to the code may improve performance depending on the specific details of the problem in hand.

A final addition is a routine to monitor each niche for signs of stagnation in a local minimum. Remedial action can be taken when this is seen to be occurring, by increasing the mutation rate, or re-initializing the population to a random starting configuration.

B. Cost Function

The cost function that we have implemented includes many of the important engineering factors which need to be considered in the overall design process. These include maximizing the homogeneity of the central region of interest (ROI) and maintaining quantities including the fringe field strength, wire volume and hoop stresses within necessary limits. Weighting factors on all of these secondary conditions must be specified with care otherwise the GA may not converge to a satisfactory design (for example the main field may tend to zero). Physical boundary conditions must also be satisfied by the design and these include both geometric constraints on magnet size and quantisation of the width and height of each coil.

Tests for exceeding the critical current density were found to be unnecessary because the requirements on hoop stresses were more severe than the constraints on the field and current densities.

Manuscript received September 24, 2001. This work is supported by a grant from EPSRC.

N. R. Shaw and R. E. Ansorge are both with the Department of Physics, University of Cambridge, UK (telephone: + 44-1223-337351, email: nrs20@phy.cam.ac.uk).

The stability of a design to build errors was also considered. A robust design is often preferable if the homogeneity of the ROI is reasonable. Stability could not be checked during optimization because of the excessive computer time required. Instead promising designs were post-processed for stability against build errors. In practice, most, but not all, designs were found to be stable against typical build errors.

C. *Efficient Field Calculations*

The accuracy of the magnetic field calculations performed throughout the optimization process depends on the region being investigated. For the central region of interest (ROI), accuracy of the order of 0.01 ppm is required. However, for the evaluation of the field at the coils for the stress calculations, an accuracy of 1% is sufficient. Similarly the fringe fields require only modest accuracy.

Three methods of magnetic field calculation are available and have been investigated:

1) Polynomial expansion and evaluation [3].
2) Forbes, Crozier and Doddrell (1997) [4].
3) Direct integration using complete elliptical integrals (CEL) [5].

The polynomial expansion of the magnetic field around the origin of the coordinate system is by far the fastest method available. It is also very accurate, using the first 16 or 18 terms in the expansion, for calculating the homogeneity of the magnetic fields over the central ROI. However, the expansion is unsuitable for calculating the field away from the central ROI, for example within current carrying coils or fringe fields, because of poor convergence. In both of these cases, an approach based on direct integration of the Biot-Savart law is required. We have examined the accuracy and relative efficiency of two methods available for this type of calculation, the Forbes and CEL methods. Following investigation, we found that the method presented by Forbes could give large errors near coil edges. The CEL method was therefore used for both the force calculations and the fringe field evaluation. The performance of these algorithms is discussed in more detail in the section III.

D. *Parallel computing*

The operation of the GA is inherently parallel, as every member of the population must have its fitness evaluated at every generation. Thus this type of calculation is eminently suitable for running on parallel clusters with many processors. We have used both inexpensive PC clusters (Beowulf) with up to 32 processors and commercial high performance computers (Hitachi SR2201 with up to 256 processors and IBM SP with up to 160 processors). The CamGASP code uses the MPI message-passing library and hence is easily ported between different parallel computer architectures. More details on MPI can be found in our previous publication and reference [6].

E. *Shimming*

Following optimization the best magnet designs were shimmed using a matrix inversion technique to calculate currents in a number of additional fixed position shim coils so as to cancel the first 5 non-zero terms in the polynomial expansion of the magnetic field potential. The use of extra shim coils additionally allows for correction of the field errors introduced in the manufacturing process and is standard practice for large MRI magnets.

III. Performance Considerations

A. *Field calculation method*

Magnetic fields in and around the current carrying, axi-symmetric coils were calculated. Comparisons were made between the method of Forbes and a direct integral method using complete elliptical integrals (CEL). In both cases a single integral must be performed numerically and we used the *qsimp* routine [7] for the evaluation of this integral. The accuracy and speed of this integration could be varied. Calculated magnetic field plots passing through a section of a single coil and along a line close to the coil edge are shown in Fig. 1.

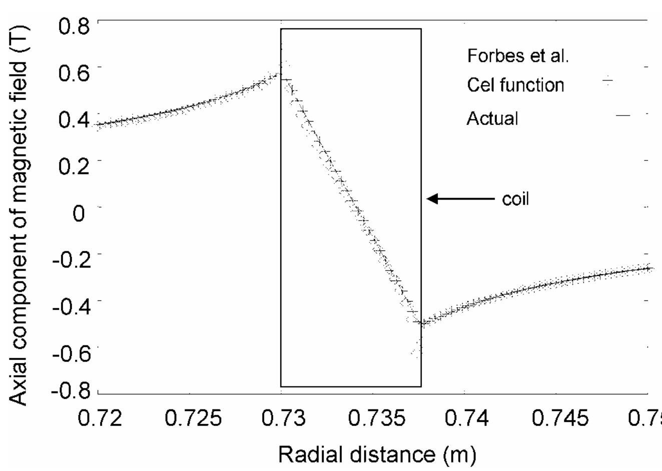

Fig. 1. Calculated magnetic field near the edge of a current carrying coil. This figure shows the results for a 0.1ms integration at each point. The CEL method gives substantially better agreement with the actual field calculated by direct integration of the Biot Savart law.

The Forbes method was found to overestimate the field at the edges of the coil by almost 25% whereas the CEL method is accurate to within 1%. Note that the time for evaluation, 0.1 ms on a Pentium II, 333 MHz processor, for the two methods is the same, so the CEL method in this case is considerably more efficient. In practice the inner edge of the coil is likely to experience the greatest hoop stress so this error in the Forbes calculation is potentially very serious. Although the accuracy of the Forbes method can be improved by allowing more computer time, this has a very detrimental effect in the context of a GA calculation where fields are repeatedly evaluated. However, when much greater fractional accuracy is required (10 ppm), the Forbes methodology appears to converge faster than the CEL method. This effect needs further investigation and may be due to rounding errors in our code.

B. GA efficiency

Another important consideration is the time taken to get the results.

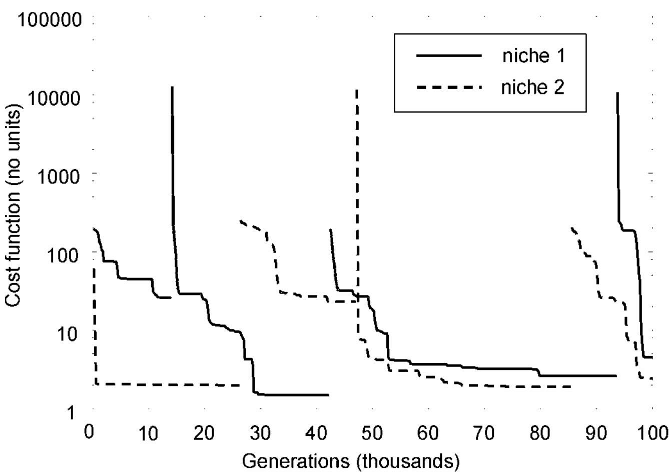

Fig. 2. Evolution of fitness function with generation number. The fitness can be seen to improve rapidly near the start of the optimization. Later, the curves flatten out as further improvements in the design become difficult. Once a niche has remained stationary for more than 2000 generations, the niche is re-initialized.

Fig. 2 shows a typical graph of best fitness versus generation for a typical run using CamGASP with stagnation monitoring. The total run lasted 8 hours and completed 100000 generations in all of 32 entirely separate niches (two of which are shown for clarity). The curves can be seen to flatten off significantly as the GA reaches a local minimum. Re-initialization of niches was performed when the fitness had not improved for the last 2000 generations.

IV. Results

A. Short-bore whole body MRI magnet

Continued pressure from clinicians has led to demand for short bore, whole body MRI magnets. This trend is as a result of the need to reduce patient claustrophobia when imaging the thorax or the head, combined with an interest in performing clinical surgery with MRI fluoroscopy. This has been matched with a general trend in industry to produce shorter bore magnets, for example the Marconi Infinion with a coil bore length of 1.26 m [8].

The design parameters for an axisymmetric, short-bore magnet were programmed into the CamGASP software. The code was then tested on a 4-node Linux PC cluster. The cost function was altered in an iterative fashion until the GA converged on reasonable solutions. The code was then ported to a massively parallel supercomputer, the Hitachi SR2201, run by the Cambridge High Performance Computing Facility. Niching was added to the genetic algorithm to gain insights into the spread of designs found.

The best designs were then post-processed using proprietary software to examine the quench properties and the effect of build-errors. Inter and intra-coil forces were calculated using a finite element package.

The design shown in Fig. 3 is a 1.0 m bore length, 1.0 m bore diameter, whole body magnet. The central field strength is a projected 1.0 T with maximum current in the windings of 110 A/mm^2.

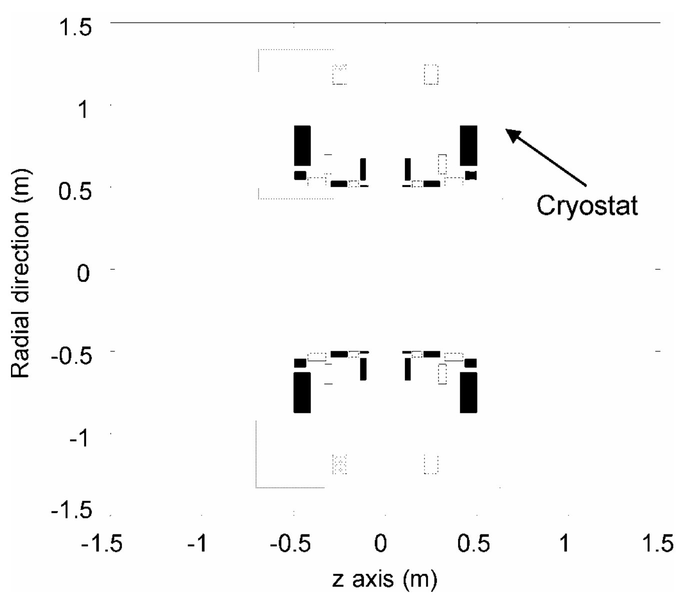

Fig. 3. Design for short whole body MRI magnet. The figure shows both positively and negatively wound coils in a slightly splayed design. The ROI spans a diameter of 300 mm with a peak-to-peak deviation of 1 to 2 ppm. The positively wound coils are shown as black and the negatively wound coils are shown as gray. The 5 pairs of superconducting shim coils are closest to the z-axis of the magnet.

The design consists of 4 main pairs of coils, producing the main magnetic field and shielding the fringe fields. A set of 5 pairs of superconducting shims was then optimized to improve the homogeneity. A further set of room temperature shims (not shown in Fig. 3), carrying a maximum of 10 A/mm^2, are located within the bore of the magnet. The uniformity across the ROI is less than +/- 0.5 ppm peak-to-peak deviation within a 300 mm sphere.

A study was undertaken on the effects of up to 0.5 mm movement in the coil positions due to manufacturing errors. It was found that the resulting non-uniformities in the magnetic field could be re-shimmed using the 5 pairs of room temperature shim coils, to produce a maximum deviation of less than 1.5 ppm peak-to-peak over the ROI. After the re-shimming process, currents in the room temperature shims were still limited to roughly 15 A/mm^2.

B. Split coil magnet for combined PET and MRI

PET (positron emission tomography) and MRI, represent two complementary imaging modalities. MRI is well known for giving high-resolution structural details of the region of interest, whereas PET focuses much more on the functional processes. The combination of these two modalities would, however, be much greater than the sum of the individual parts. By separating the two halves of a conventional cylindrical MRI magnet, a PET detector array can be installed in the region of relatively low magnetic field between the two sides. Either shielded PMTs (photo multiplier tubes) or APDs (avalanche photo diodes) are possible choices for the PET detector. This approach is in contrast to a previous attempt in which the PET detector was placed entirely within the bore of a conventional MRI magnet and long fiber optics were used to transport light to remote PMTs [9].

For our optimization, various combinations of the coil separation and the size of the ROI were examined using niching to look at a wide spectrum of possible designs.

Preliminary results show that a ROI of 70 to 90 mm is feasible with a coil separation of 100 to 200 mm and a peak-to-peak deviation of 1 to 2 ppm. A typical magnet configuration is shown in Fig. 4, although the details are still to be finalized.

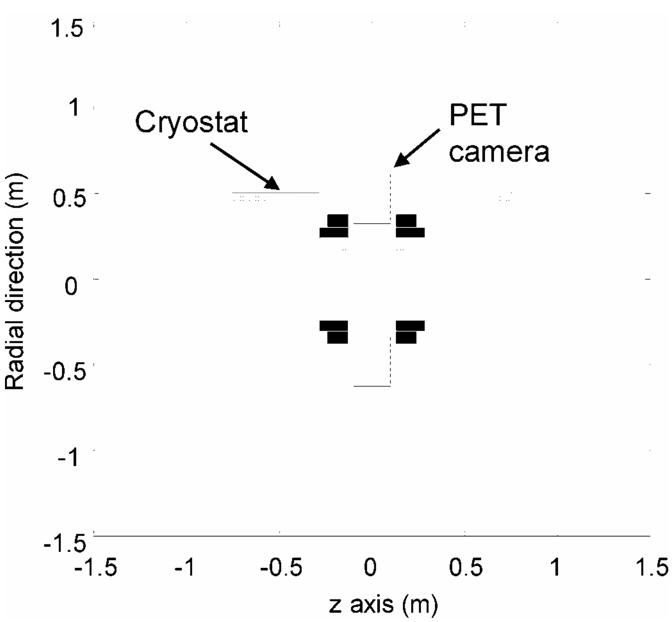

Fig. 4. Design for split coil MRI magnet with PET camera installed in a low field region between the coils. The field strength is 3.0 T, with 2 ppm peak-to-peak deviation over a ROI of diameter 70 mm.

V. Conclusions

We have presented in this paper a flexible approach for designing novel magnets. The CamGASP software is easy to use and alter for different design tasks. Many of the GA parameters are implemented as run-time variables and the design specific routines are modular and written in C.

Although GAs have been shown to avoid entrapment in many local minima, from the study of multiple niching, it has become clear that even after many thousands of generations, the optimization routine will not converge on a single, global minimum unless the search space is reasonably small.

Combining genetic algorithms with simulated annealing may in the end be the best way forward, the genetic algorithms to find a selection of attractive local minima, whilst the simulated annealing quickly optimizes the local search.

With further refinement, GAs should continue to offer an excellent design tool for complex design problems particularly with the continual increase in computational resources. In the two years since our last paper, PC processors have gone from a typical 300 MHz to 2 GHz, which clearly indicates great promise for the future.

VI. Acknowledgment

The help of the University of Cambridge High Performance Computing facility is acknowledged for use of the SR2201 and IBM SP and for general support. The 4-node Linux cluster was purchased with the aid of a Royal Society grant.

VII. References

[1] R. E. Ansorge, T. A. Carpenter, L. D. Hall, N. R. Shaw, G. B. Williams, "Use of parallel supercomputing to design magnetic resonance systems," *IEEE Trans. Appl.. Superconduct.*, vol. 10, pp 1368-1371, 2000
[2] V. M. Kureichik, "Genetic algorithms: state of the art, problems, and perspectives," *Journ. of Comp. and Sys. Sci. Int*. Vol 38, pp. 137-152, 1999
[3] M. W. Garrett, "Axially symmetric systems for generating and measuring magnetic fields, Part I," J. of Appl. Phys. Vol 22 (9), pp 1091-1107, September 1951.
[4] L. K. Forbes, S. Crozier, D. M. Doddrell, "Rapid computation of static magnetic fields by thick circular solenoids," *IEEE Trans. on Magnetics*, Vol. 33, pp 4405-4410, Sept. 1997.
[5] R. Bulirsch, "Numerical calculations of elliptic integrals and elliptic functions. III," Numerische Mathematik, Vol 13, pp 305-315, 1969.
[6] J. Bruck et al., "Efficient Message Passing Interface (MPI) for parallel computing on clusters of workstations," Journal of Parallel and Distributed Computing, vol. 40, pp. 19-34, 1997.
[7] W. H. Press, S. A. Teukolsky, W. T. Vetterling, B. P. Flannery, *Numerical Recipes in C*, 2nd ed., Cambridge University Press, 1995.
[8] F. Davies, G. Demeester, D. Melotte, M. Morich, A. Thomas, "Short magnets for whole-body magnetic resonance imaging," Conf. Proc. ISMRM 2001, 1149
[9] Y Shao et al., "Simultaneous PET and MR imaging," *Phys. Med. Biol.*, Vol. 42, pp 1965-1970, 1997.